15TH IEA HEAT PUMP CONFERENCE
MAY 26–29, 2026 | HOFBURG
VIENNA 2026
DECARBONISATION THROUGH INNOVATION

Redesign a thermodynamic heat recovery unit with R290: experimental and simulation results

Sara Bordignon[a,*], Francesco De Zan[a], Alessandro Carlesso[b], Simone Piovesan[a], Stefano Bortolin[b], Marco Azzolin[b]

[a]Clivet SPA, Feltre, Via Camp Lonc, 25, 32032 Z.I. Villapaiera, Italy
[b]University of Padova, Padova, Via Venezia, 1, 35131, Italy

Abstract

Proper ventilation systems are critical for providing high Indoor Air Quality standards in buildings. Concerning nearly zero energy buildings (NZEB), and in renovated buildings, the energy impact of mechanical ventilation units on the overall consumption is significant. In this context, thermodynamic heat recovery units have a great potential to decrease the electrical energy demand and contribute to improving the indoor thermal comfort and meet space heating and cooling loads. Thermodynamic heat recovery units are recuperators provided with an internal vapor compressor cycle whose function is to enhance the supply airflow temperature by exploiting the energy content of the exhaust airflow extracted from the building. In this way, the system can be used to efficiently meet a part of the heating and cooling loads, integrating the existing generation system. Towards global targets of net zero emissions, the redesign of many vapor-compression cycle units, converting them from synthetic refrigerants to natural refrigerants represents both an opportunity and a challenge for manufacturers. In particular, when it comes to the use of hydrocarbons, the main challenge for manufacturers is to provide the same performance of a synthetic refrigerant unit, with a maximum refrigerant charge of 150 g to comply with current safety regulations (IEC 60335-2-40).
This paper aims to investigate the redesign of an existing R32 thermodynamic heat recovery unit to R290 refrigerant. The casing of the unit is kept the same size as the original, due to spacing requirements, and attention is given to the refrigeration cycle. Experimental tests are performed to assess the performance. A numerical model was developed in MATLAB to reproduce the steady-state behavior of the unit under different thermodynamic conditions and operating configurations. The model was then validated using experimental data, showing good accuracy.

Selection and/or peer-review under the responsibility of the organizers of the 15th IEA Heat Pump Conference 2026.

Keywords: Heat Recovery Unit; R290; Natural Refrigerants, Mechanical Ventilation

1. Introduction

Mechanical ventilation is crucial for healthy indoor air quality and occupant safety and comfort, especially in the post-COVID era, by mitigating airborne disease transmission and ensuring regulatory compliance. In 2020, 28 million continuously operating ventilation units (VUs) were in use in EU27 (not including intermittently operating exhaust fans in e.g. toilets or bathrooms). Of these, 20 million VUs (71%) were for residential use, servicing 25% of the EU27 residential dwelling area [1]. For sustainable building operations, it is clear that these units must be energy-efficient, together with the importance of recovering the thermal energy from the exhaust air flows. Thermodynamic heat recovery is key, as it recovers thermal energy from exhaust air to pre-condition fresh air, significantly reducing energy consumption, lowering operating costs, and contributing to environmental sustainability through carbon emissions mitigation.
Along with energy efficiency and in the context of the European F-gas Regulation [2], the usage of natural

[1*] Corresponding author. *E-mail address:* s.bordignon@clivet.it

refrigerants plays a role in stand-alone heat pump equipment with a maximum rated output lower than 12 kW. The regulation requires these systems to adopt refrigerants with a GWP lower than 150, effective 2027. A stricter limit takes effect in 2032, permitting only non-fluorinated refrigerants for monobloc heat pumps and air conditioning units up to 12 kW. Within this regulatory framework, the adoption of propane (R290) as a natural refrigerant is a good option, although presenting significant challenges for manufacturers. The main challenge lies in developing systems that can match the performance of those using synthetic refrigerants, all while adhering to the current safety IEC 60335-2-40:2024 standard [3], which limits the refrigerant charge to 150 g without imposing further installation limitations.
This study aims to examine the operating behavior and potential performance improvements of a reversible mechanical ventilation unit using R290, compared to an equivalent configuration charged with R32, while keeping under control the refrigerant charge limitation. A previous work conducted on a similar unit [4], reports some thermodynamic analysis performed with Coil Designer [5] and Simcenter Amesim [6], though highlighting some difficulties in matching the experimental data. In this second work, the experimental set up allowed a better focus on the finned coil heat exchangers. The research combines experimental testing with the development of a numerical simulation model in MATLAB [7], designed to reproduce the steady-state operation of the unit under a variety of thermodynamic conditions and operating configurations, and previously investigated in Guzzardi et al. [8].

2. Thermodynamic heat recovery unit and experimental setup

A thermodynamic heat recovery unit is an active recovery system that uses a vapor compression cycle to increase the temperature of the supply air using the thermal energy contained in the exhaust air extracted from the building. These devices combine the functions of controlled mechanical ventilation with those of a heat pump, ensuring air exchange and, at the same time, efficiently covering part of the heating and cooling loads, integrating with the existing generation system. The performance can be evaluated by a coefficient of performance (COP), which is calculated as the cooling or heating capacity measured between the inlet and the outlet of the supply duct, divided by the total electrical power absorbed by the unit (including the compressor, fans, electrical board). Unlike traditional heat pumps, thermodynamic recovery units exploit a more stable and favorable heat source, as the exhaust air maintains a constant temperature, independent of external climatic variations. This allows for enhanced performance, with a COP in heating mode that increases as outside temperatures decrease, unlike conventional heat pumps.
The unit, shown in Figure 1, consists of:

- Supply duct (9-6) equipped with air treatment finned round tube heat exchanger, to supply fresh air into the building;
- Return duct (7-10) equipped with air source finned round tube heat exchanger, to remove extract exhaust air from the building.

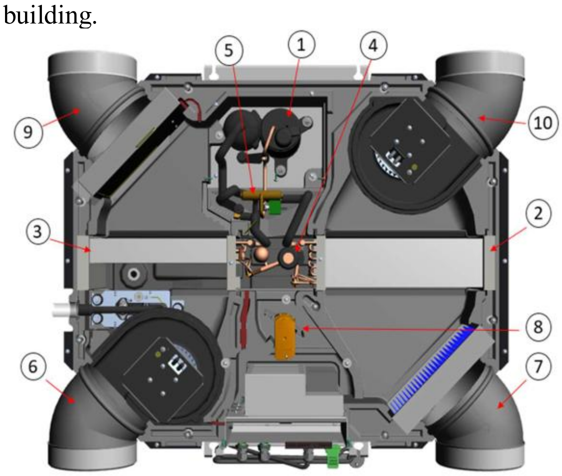

Figure 1: System layout. 1: compressor, 2: air source coil, 3: air treatment coil, 4: expansion valve, 5: 4-way valve, 6: supply duct (with radial fan), 7: return duct (with air filter), 8: air damper; 9: suction duct (with air filter); 10: expulsion duct (with radial fan)

In the cold season the air source coil absorbs heat from outgoing exhaust air, causing refrigerant to evaporate while the air treatment coil releases heat to incoming fresh air, condensing refrigerant back into liquid phase. In the warm season, the system can invert its cycle by means of a 4-way valve, extracting heat from incoming air to heat the outgoing air. Components wise, the air circuits are equipped with radial fans and air filters ,
the compressor is inverter driven and an automatic damper is installed in the return air duct in order to manage

the load difference to the fin and coils heat exchangers among the different seasons.
The experimental test rig used in this study is shown in Figure 2. The apparatus is equipped with a series of sensors for measuring temperature (indicated as *T* in the figures), relative humidity (*RH*), and volumetric air flow rate (*fr*) of the *supply* and *exhaust* channels. These instruments are installed at the inlets (*in*) and outlets (*out*) of the ducts, as well as inside the unit, to characterize the thermodynamic behavior of both the air and refrigerant circuits. Pressure sensors measure the absolute pressure (P_{abs}) at the inlet and outlet of each channel, and two compensation fans are used to set an air pressure difference (*Dp*) to 50 Pa. Sensors positioned along the air paths allow the sensible and latent heat exchange to be determined, while thermocouples mounted on the heat exchangers provide information on the operating conditions of the refrigerant. The heat exchangers are provided with thermocouples at the inlet and outlet of all refrigerant circuits, and in the middle of some the circuit (on the curves) to derive the condensation and evaporation temperatures. Figure 2 (b) illustrates the placement of the thermocouples used to measure the air temperature inside the unit. Specifically, four sensors at the source and treatment finned coil outlets, along with four sensors at the inlet of the source finned coil, are designated as $T_{S,air,out}$, $T_{T,air,out}$ and $T_{S,air,in}$, respectively. The sensor $T_{air,circ}$ is located in the center of the unit to monitor the air temperature within the piping area, while $T_{air,damp}$ measures the temperature near the damper. Finally, $T_{comp,in}$ and $T_{comp,out}$ are thermocouples positioned at the compressor's inlet and outlet; these are mounted in direct contact with the piping and are fully insulated. Condensate weight is also measured.

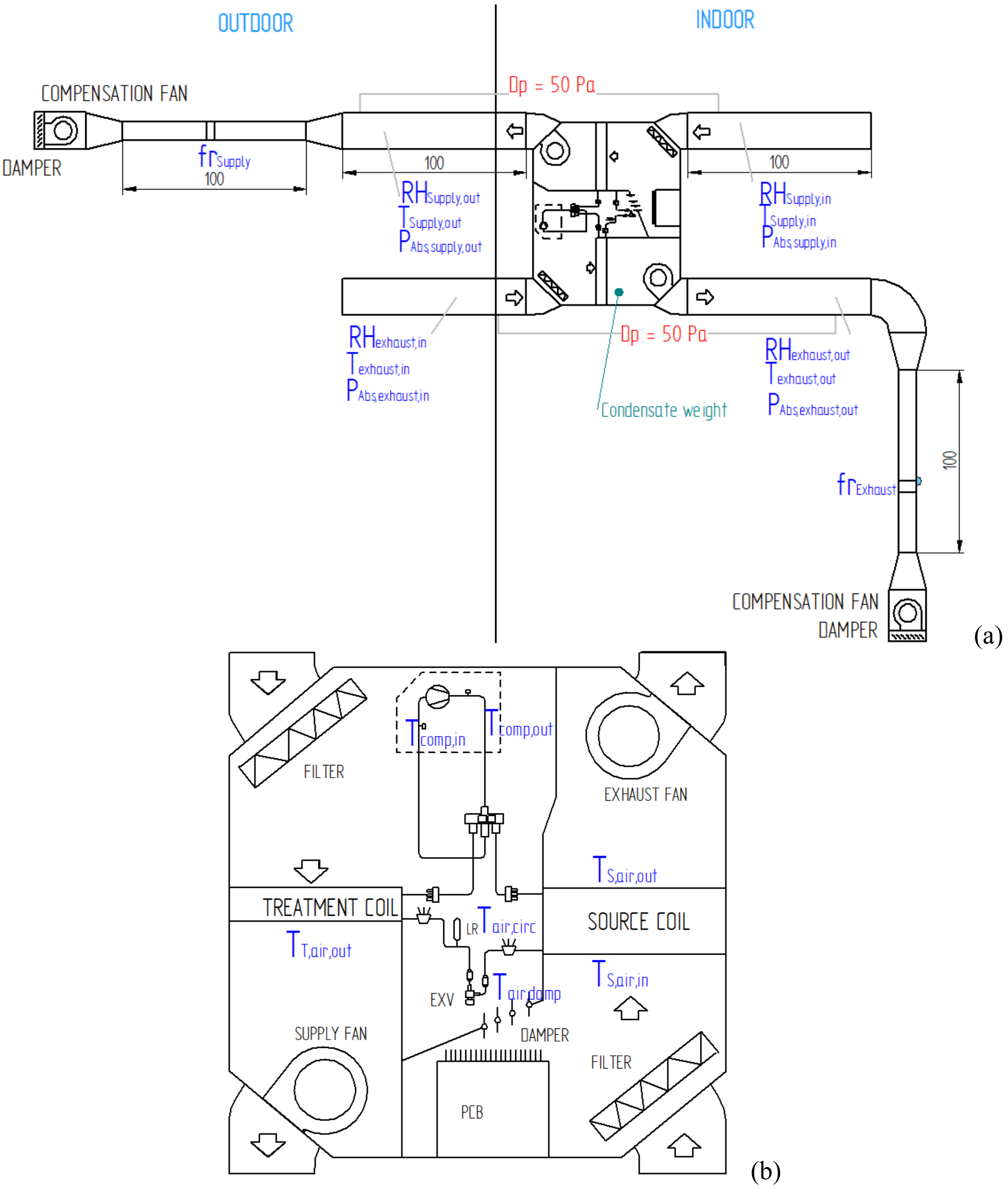

Figure 2: Schematic of the test rig – air measurements outside the unit (a) and in the unit (b).

Data acquisition was performed automatically once steady state conditions were reached, with measurements recorded at regular intervals and subsequently processed for performance evaluation. Both units were pre-charged with their respective refrigerants. The unit charged with propane is equipped with a compressor and 4 way and expansion valves specifically designed for this refrigerant. The internal volume of the heat exchangers is around 185 cm^3 for the treatment coil and 410 cm^3 for the source coil, while the internal volume of the rest of the refrigerant circuit components is around 395 cm^3.

3. Experimental results

The target of the tests was to compare the performance of the R290 unit with the existing one working with R32, limiting the propane charge to 150 g. Tables 1 and 2 compare the test results between R32 and R290: for the sake of brevity, only one condition in heating and cooling mode is reported.

Table 1: Results comparison between unit R290 and R32: heating (Outdoor Temperature 7 °C Dry Bulb/6°C Wet Bulb, Indoor Temperature 20°C D.B./13.7°C W.B.)

Parameter	R32 Unit	R290 Unit	Deviation
Heating capacity [kW]	1.97	1.97	0%
Power consumption [kW]	0.43	0.43	0%
Condensation Temperature [°C]	37	36.4	-0.6°C
Evaporation Temperature [°C]	4.4	5.0	+0.6°C
$COP_{heating}$ [kW/kW]	4.58	4.55	-0.7%

Table 2: Results comparison between unit R290 and R32: cooling (Outdoor Temperature 35 °C D. B./24°C W.B., Indoor Temperature 27°C D.B./19°C W.B.)

Parameter	R32 Unit	R290 Unit	Deviation
Cooling capacity [kW]	1.88	1.87	-0.5%
Power consumption [kW]	0.57	0.56	-1.8%
Condensation Temperature [°C]	51.0	51.5	+0.5°C
Evaporation Temperature [°C]	14.6	12.9	-1.7°C
$COP_{cooling}$ [kW/kW]	3.29	3.31	+0.6%

Despite its different configuration and lower refrigerant charge, the R290 unit delivers the comparable performances of R32.

4. Modelling of the heat exchangers and comparison with the experimental data

The simulation model was developed in MATLAB to replicate the thermodynamic and heat transfer processes that occur within the unit's components. The model adopts a finite volume approach to discretize the heat exchangers into a series of elementary control volumes, as shown in the Figure 3, where local mass and energy balances are solved. Each discretized element is treated as an individual heat exchanger, with heat and mass transfer processes evaluated using the ε-NTU method and well-established correlations from the literature for heat transfer coefficients and pressure drops calculations (see Table 3). In previous studies, the dependence of the results on the number of discretization elements was analyzed [8]. Based on those findings, the number of longitudinal elements adopted in the present work was selected, equal to 3 per tube. Refrigerant properties are obtained from the Refprop 10 database [8], while air properties are derived from psychrometric relationships.

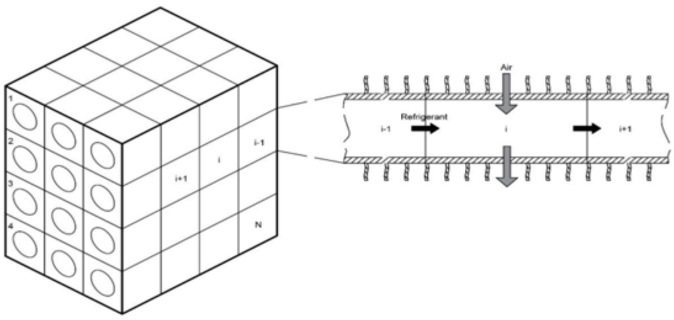

Figure 3: Discretisation of the finned coil heat exchanger with the i-th element [1]

Table 3: Heat transfer coefficients and pressure drop correlations used

	Heat transfer coefficient	Pressure drop
Air	Wang et al. [10] Sadeghianjahromi and Wang [11]	Wang et al. [10] Sadeghianjahromi and Wang [11]
Single-phase refrigerant	Gnielinski [12]	Churchill [13]
Two-phase refrigerant	Condenser: Cavallini et al. [14] Evaporator: Diani et al. [15] Vapor quality at the dry-out: Padovan et al. [16]	Condenser: Friedel- Rohuani [17] [18] Evaporator: Friedel-Rohuani [17] [18]

In addition to the exchangers, the model structure includes representations of the air circuit, compressor, and expansion device. For the compressor, ARI polynomial correlations (from the manufacturer) are used to calculate the mass flow rate, while the expansion valve is modeled as an ideal component. Regarding air, it is represented by dividing the flow across the heat exchanger into several sections, corresponding to the rows and circuits of the refrigerant. Within each section, it is assumed that the thermodynamic properties of the air, i.e. temperature, enthalpy and specific humidity, are uniform. The calculation proceeds sequentially, updating the state of the air after each row based on heat exchanges with the refrigerant. A distinction is made between the behavior of the condenser, where humidity remains constant, and that of the evaporator, where it can vary due to condensation.
An example of the air circuit is shown in Figure 4, which highlights for one circuit, the temperature distribution by row. The sequence of rows, as well as the number of elements per row, depends on the path of the refrigerant circuit.

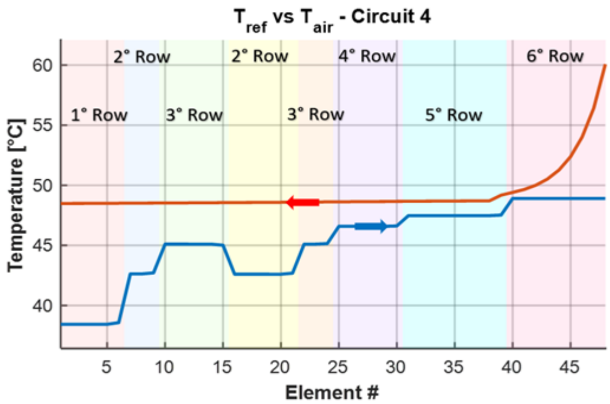

Figure 4: Refrigerant-air temperature variation inside the condenser in cooling mode for the circuit 4. Air temperature in orange, refrigerant flow in blue.

Two main types of simulation were implemented to model the thermodynamic heat recovery unit, which differ mainly in complexity and purpose. *Type 1* simulations, whose operation is described in the flow chart of Figure 5, uses iterative procedures to determine condensation and evaporation temperatures based on the imposed values of subcooling and superheating. Using the secant method, the model iteratively adjusts these temperatures until the calculated enthalpies match those desired to achieve the desired superheating and subcooling. This approach allows the model to predict the thermodynamic behavior of the system under varying operating conditions.

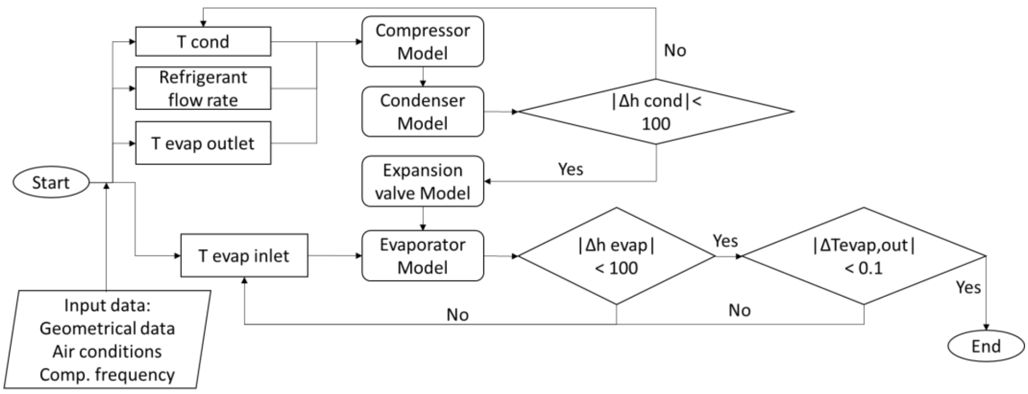

Figure 5: Type 1 model algorithm

In contrast, *Type 2* simulations directly impose condensation and evaporation temperatures as input data, avoiding iterative temperature calculation. This simplifies the numerical process, reduces computation time, and ensures faster convergence. *Type 2* models are mainly used for validation, comparing simulation results with experimental data to verify the accuracy of the correlations and assumptions implemented.
The input and output variables of *Type 2* models vary depending on the operating mode (heating or cooling), particularly with regard to the direction of air flow relative to the refrigerant. In heating mode, the air flows parallel (cocurrent) to the refrigerant, while in cooling mode it flows in the opposite direction (counter current). Consequently, during cooling simulations, the inlet air temperature was adjusted iteratively to ensure consistency with the measured temperature.
Using the geometric characteristics and thermodynamic properties of both the air and refrigerant entering the heat exchanger as boundary conditions, the models predict the corresponding outlet conditions, as well as the heat exchanger capacity and superheat and subcooling values. The results of these simulations were then compared with experimental data to assess the reliability of the model.

4.1. Heating mode - R290

Figures 6 to 8 show a comparison between calculated and experimental values for heat transfer capacities, air parameters, and refrigerant subcooling and superheating values. The results show deviations in heat transfer capacities within 5% and differences in temperatures and subcooling and superheating values of less than 2 °C. Among the various factors that may affect them present results, the most significant are air-side and/or refrigerant-side maldistribution. However, these results are acceptable, also given that the capacity is measured on the air side, which intrinsically leads to higher uncertainties, mainly related to the relative humidity and airflow measurements, and confirm that the model is capable of reproducing the actual behavior of the system. The results refer to different test data and are presented for a specific frequency of the compressor and opening of the expansion valve. For example 50 Hz – 320 means a test point at 50 Hz of the compressor and 320 steps of the expansion valve opening. The operating conditions for all the heating tests here presented are: outdoor temperature 7 °C D.B./6°C W.B., indoor temperature 20°C D.B./13.7°C W.B.

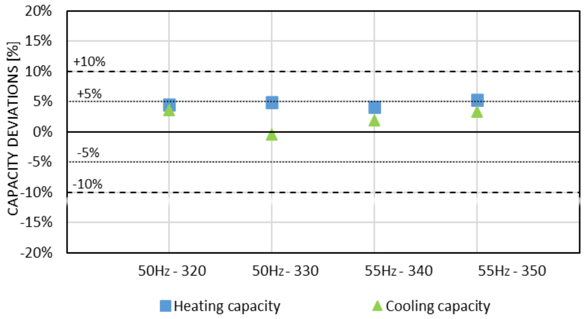

Figure 6: Deviation ratio between calculated and experimental heat transfer capacities in the condenser and evaporator

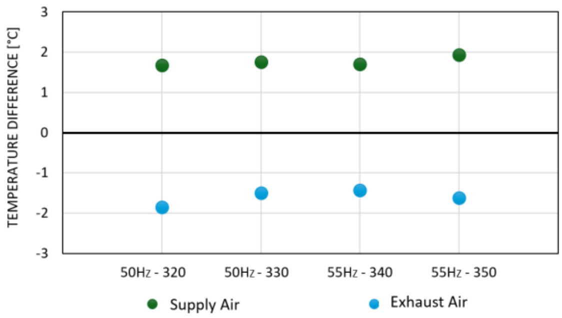

Figure 7: Deviation between calculated and experimental air parameters

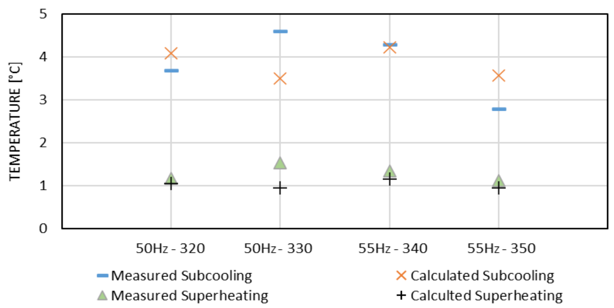

Figure 8: Calculated and experimental subcooling and superheating values

A detailed comparison between the measured and simulated temperatures of the refrigerant and air is shown in Figures 9 and 10. The comparison is based on the thermal profiles generated by the model, which describe the temperature trends of the refrigerant and air along the condenser and evaporator. The experimental data are shown as points, with the refrigerant temperature in orange and the air temperature in blue, allowing for an immediate assessment of the coherence between simulation and measurements.
The results demonstrate a good agreement between the model predictions and the experimental data, with a maximum deviation of ±2 °C. These results further confirm the reliability of the model in heating mode.

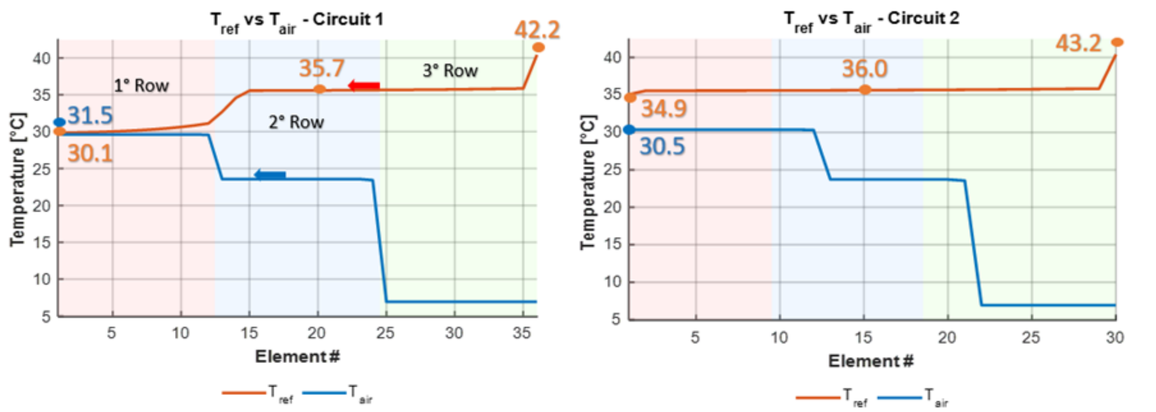

Figure 9: Comparison between the refrigerant (blue - T_{ref}) and air (orange - T_{air}) temperatures obtained from the model and experimental data at the condenser (50Hz - 320)

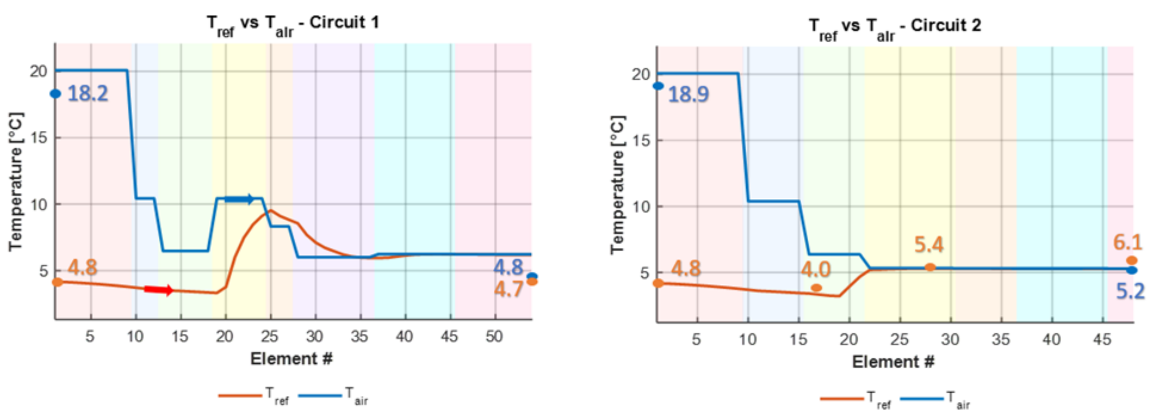

Figure 10: Comparison between the refrigerant (blue - T_{ref}) and air (orange - T_{air}) temperatures obtained from the model and experimental data at the evaporator (50Hz - 320 test)

4.2 **Cooling mode - R290**

Figures 11 to 13 compare the experimental and simulated results for the cooling mode. Although the model shows slightly larger deviations than in the heating mode, the overall accuracy remains good. The deviations in heat transfer capacity are in the order of 5%, and the temperature values, including subcooling, and superheating values differ by less than 2°C. The operating conditions for all the cooling tests here presented are: outdoor temperature 35 °C D.B./24°C W.B., indoor temperature 27°C D.B./19°C W.B.

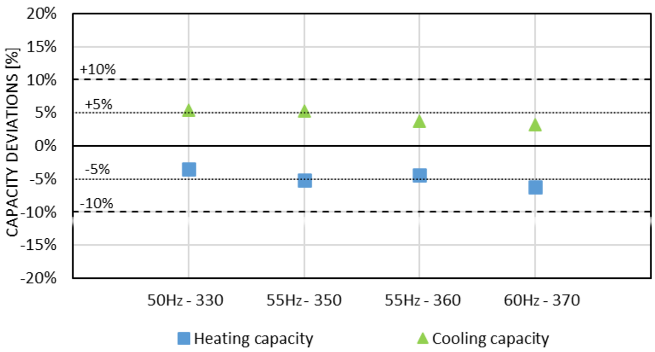

Figure 11: Deviation ratio between calculated and experimental heat transfer capacities in the condenser and evaporator

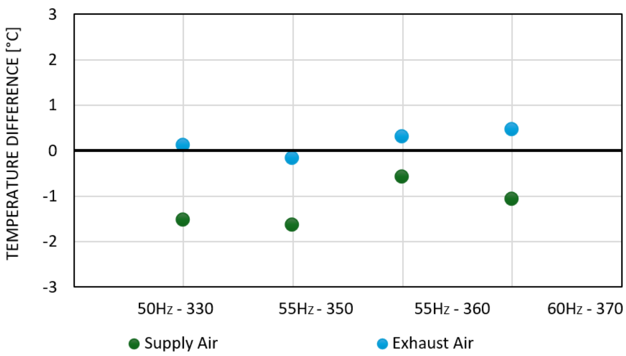

Figure 12: Deviation between calculated and experimental air parameters

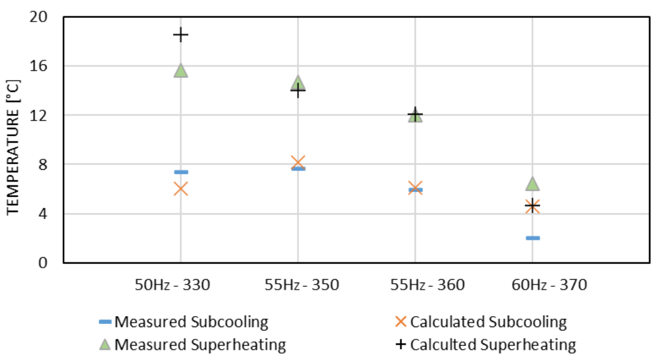

Figure 13: Calculated and experimental subcooling and superheating values

These deviations can be mainly assigned to the non-uniform distribution of the refrigerant between the circuits observed during the experimental campaign. This discrepancy can also be found in the results of the model itself, as a result of the different lengths of the circuits. The deviation at the condenser can be associated with uncertainties in the measurement of the air temperature at the inlet of the source coil: with the damper open, the source heat exchanger airflow is the result of the airflows coming from the indoor and outdoor environments, thus altering the actual inlet temperature. Since the bypass air flow is not measured directly, but only values at the outlet ducts are measured, this introduces uncertainty in the condenser inlet conditions and,

consequently, in the calculated heat capacity.
A further comparison between the measured and simulated temperature profiles for both air and refrigerant is shown in Figures 14 and 15. The results indicate that, also for cooling model, maximum deviations in temperatures are around 2 °C, and that the general temperature trends are consistent with experimental observations.

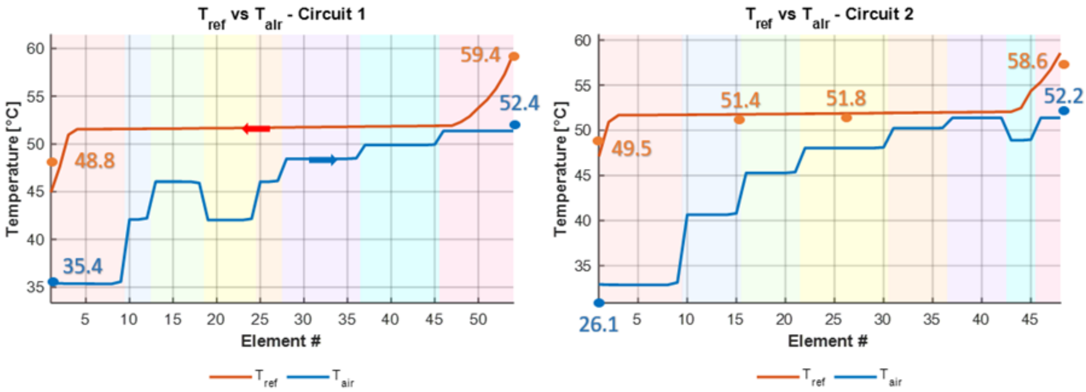

Figure 14: Comparison between the refrigerant (blue - T_{ref}) and air (orange - T_{air}) temperatures obtained from the model and experimental data at the condenser (60Hz - 370)

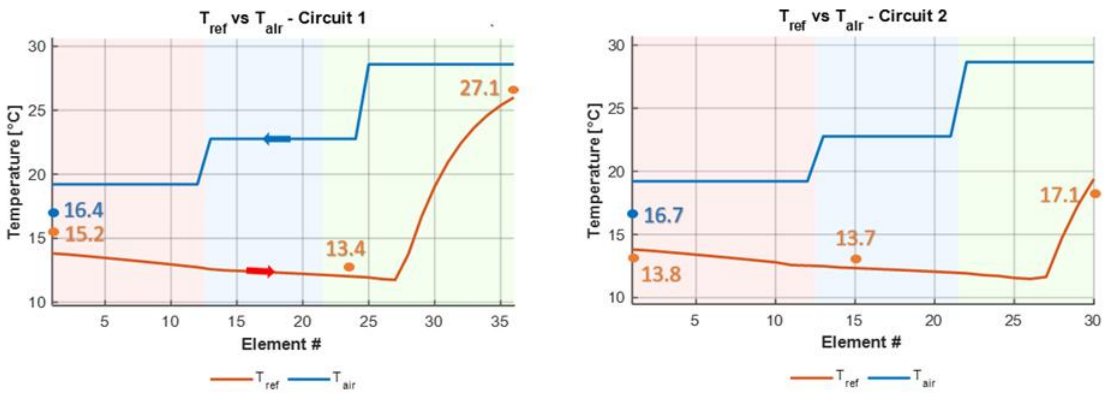

Figure 15: Comparison between the refrigerant (blue - T_{ref}) and air (orange - T_{air}) temperatures obtained from the model and experimental data at the evaporator (60Hz - 370)

5. Total temperature penalization analysis

To conduct a comprehensive comparison between refrigerants, both their heat transfer coefficients and pressure drop characteristics must be considered. The TTP method proposed by Cavallini et al. [9] introduces two performance evaluation criteria (PECs)—the penalty factor (PF) and the total temperature penalty (TTP)—specifically for this purpose. These criteria allow assessing the potential heat transfer performance of refrigerants during condensation in both smooth and enhanced tubes. PF and TTP are closely related and incorporate two key penalization terms that are critical in condensation processes: one associated with the driving temperature difference for heat transfer, and the other accounting for the temperature decrease caused by pressure drop. The latter indirectly influences heat transfer by modifying the driving temperature difference along the refrigerant path. Cavallini et al. have also demonstrated that the TTP and PF are equivalent to the entropy generation and exergy losses.

The PF parameter considers the driving temperature difference (ΔT_{dr}, saturation temperature minus wall temperature) and saturation temperature decrease associated with the frictional pressure drop (ΔT_{sr}), which causes a decrease in its saturation temperature (ΔT_{si}). The formula used to calculate the PF is presented in Equation (1). The PF parameter can be used as a quantitative criterion to rank the heat transfer performance of different fluids: when given the same value of HTC and pipe geometry, the smaller the PF, the better the performance potential of the refrigerant.

$$PF = \Delta T_{sr} \cdot \Delta T_{dr} \quad (1)$$

The TTP parameter combines the two penalties as follows:

$$TTP = \Delta T_{dr} + 0.5\Delta T_{sr} \quad (2)$$

By considering that only about one-half of the refrigerant saturation temperature drop is lost as heat transfer driving potential.

The TTP parameter is particularly useful for optimizing the length of condenser circuits. In fact, the optimal circuit length closely corresponds to the condition at which the TTP reaches its minimum. In the design of a finned-coil condenser, once the overall geometry, the total thermal capacity, and the operating conditions of the secondary fluid have been fixed, the designer retains essentially a single degree of freedom: the number of parallel refrigerant circuits (assuming all circuits have identical tube-pass lengths). A reduction in the number of circuits increases the length of each circuit, which means that the same total mass flow rate of refrigerant is distributed over fewer circuits. As a result, the higher the mass flow in each tube, the higher the refrigerant heat transfer coefficient and thus the lower will be the necessary driving mean temperature difference (ΔT_{dr}). However, this improvement is counterbalanced by an increase in friction pressure losses due to longer circuits and higher velocities, resulting in a higher drop in saturation temperature (ΔT_{sr}) along the refrigerant circuit (and this affects the driving temperature difference). The minimum value of the TTP corresponds to the optimal circuit length (L_{opt}) that minimizes the exergy losses at the given operating conditions.

In the present case, he TTP method was applied to the condenser under investigation to determine, from an exergy-based perspective, the optimal circuit length when operating with R32 and R290. A dedicated MATLAB model was developed to compute the TTP for each refrigerant and, consequently, the corresponding optimal circuit length, given the overall condenser geometry (internal tube diameter equal to 4.5 mm), heat flux equal to 4 kW/m^2, and secondary fluid operating conditions. The refrigerant-side heat transfer coefficient was evaluated using Cavallini's correlation [11], while frictional pressure drops were predicted with the Friedel and Rouhani correlations. The TTP was evaluated over a range of refrigerant mass flow rates—thus exploring different circuit lengths—and the results are shown in Figure 16. For R32, the optimal circuit length is 9.3 m, corresponding to a minimum TTP of 0.44 K. For R290, the optimal length is significantly shorter, 4.9 m, with a minimum TTP of 0.68 K. This indicates that, under the considered operating conditions, R32 exhibits lower exergy losses and allows for longer circuits due to its lower pressure drop, whereas R290 requires shorter circuits, implying a higher number of parallel refrigerant circuits. However, as can be noted from the figure, consistent with the observations of Cavallini et al. [10], the TTP curve can exhibit a relatively flat minimum. This means that the exact value of L_{opt} is not critical: small deviations from the optimum have only a marginal effect on overall performance. The condenser tested experimentally features circuit lengths of 7.6 m for the first circuit and 6.8 m for the remaining ones, which fall within the range predicted by the TTP analysis.

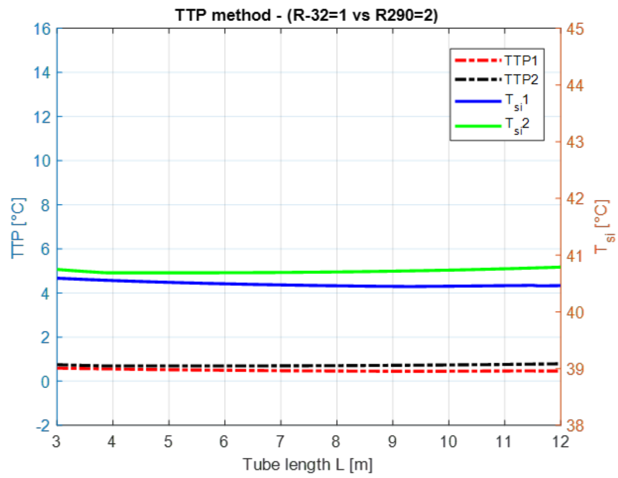

Figure 16: Total temperature penalization parameter (TTP), Refrigerant saturation temperature (T_{si}) over the tube length, when applying the PEC analysis to R32 and R290 to a finned coil condenser.

1. Conclusions

This study examined the redesign and performance of a reversible thermodynamic recovery unit originally developed for R32 and subsequently adapted to operate with R290, in accordance with the strict 150 g charge limit required by IEC 60335-2-40. The results show that, despite this constraint, the R290 unit can achieve performance comparable to those of the R32 reference system and, under certain operating conditions, even exceed them. A numerical model was developed in MATLAB to reproduce the steady-state behavior of the unit under different thermodynamic conditions and operating configurations. The model was then validated using experimental data. The validation showed that it is capable of capturing the overall thermal behavior of the system with good accuracy. The deviations between the simulated and measured values remained within acceptable limits. Slightly larger deviations appeared in cooling mode. These were partly caused by the non-uniform distribution of the refrigerant between the circuits and uncertainties in the conditions of the air entering the condenser. Overall, the results confirm that the model is capable of representing the actual operation of the unit and can serve as a useful tool for future improvements and optimizations of the system. However, the model is based on purely steady-state assumptions. It is therefore unable to reproduce dynamic phenomena such as local variations in air temperature, humidity, or air flow rate. Further calibration, as well as greater knowledge of the air-side heat transfer coefficient, could improve model performance, especially if supported by a more detailed characterization of the air and refrigerant profiles. Increasing the longitudinal discretization beyond the current three segments could also improve the representation of local effects, although it would increase numerical complexity.

References

[1] European Commission, «Ventilation Units,» 2024. [Online]. Available: https://energy-efficient-products.ec.europa.eu/product-list/ventilation-units_en#consumers-1. [13 November 2025].

[2] European Parliament and Council of European Union, *Regulation (EU) 2024/573 of the European Parliament and of the Council of 7 February 2024 on fluorinated greenhouse gases,* 2024.

[3] International Electrotechnical Commission, *Household and similar electrical appliances – Safety – Part 2-40: Particular requirements for electrical heat pumps, air-conditioners and dehumidifiers, IEC 60335-2-40:2024,* Geneva, Switzerland, 2024.

[4] B. Mirko, P. Simone, R. Paolo, N. Yuri e A. Andrea, «Development of a residential thermodynamic active mechanical ventilation machine working with propane,» in *16th IIR Gustav Lorentzen Conference on Natural Refrigerants*, College Park, Maryland, USA, 2024.

[5] J. Haobo, A. Vikrant e R. Reinhard, «CoilDesigner: a general-purpose simulation and design tool for air-to-refrigerant heat exchangers,» *International Journal of Refrigeration,* vol. 29, pp. 601-610, 2006.

[6] Siemens Digital Industries Software, *Simcenter Amesim,* Plano, TX, USA, 2024.

[7] The MathWorks, Inc., *MATLAB,* Natick, MA, USA, 2024.

[8] C. Guzzardi, M. Azzolin e S. D. C. D. Lazzarato, «Refrigerant mass distribution in an invertible air-to-water heat pump: effect of the airflow velocity,» *International Journal of Refrigeration,* vol. 138, pp. 180-196, 2022.

[9] E. W. Lemmon, I. H. Bell, M. L. Huber e M. O. McLinden, *NIST Standard Reference Database 23: Reference Fluid Thermodynamic and Transport Properties—REFPROP, Version 10.0,* Gaithersburg: National Institute of Standards and Technology, Standard Reference Data Program, 2018.

[10] C. C. Wang, J. Y. Jang e N. F. & Chiou, «A heat transfer and friction correlation for wavy fin-and-tube heat exchangers,» *International Journal of Heat and Mass Transfer,* vol. 31, p. 808–813, 1998.

[11] A. Sadeghianjahromi e C.-C. Wang, «Heat transfer enhancement in fin-and-tube heat exchangers – A review on different mechanisms,» *Renewable and Sustainable Energy Reviews,* vol. 137, 2021.

[12] V. Gnielinski, «On heat transfer in tubes,» *International Journal of Heat and Mass Transfer,* vol. 63, pp. 134-140, 2013.

[13] S. Churchill, «Friction factor equation spans all fluid regimes,» *Chemical Engineering,* vol. 84, pp. 91-92, 1977.

[14] A. Cavallini, D. Del Col, S. Mancin e L. & Rossetto, «Condensation of pure and near-azeotropic refrigerants in microfin tubes: A new computational procedure,» *International Journal of Refrigeration,* vol. 32, pp. 162-174, 2009.

[15] A. Diani, S. Mancin e L. Rossetto, «R1234ze(E) flow boiling inside a 3.4 mm ID microfin tube,» *International Journal of Refrigeration,* vol. 47, p. 105–119, 2014.

[16] A. Padovan, D. Del Col e L. & Rossetto, «Experimental study on flow boiling of R134a and R410A in a horizontal microfin tube at high saturation temperatures,» *Applied Thermal Engineering,* vol. 31, p.

3814–3826, 2011.

[17] L. Friedel, «Improved friction pressure drop correlations for horizontal and vertical two phase pipe flow,» *European Two Phase Flow Group Meeting, Ispra, Italy,* 1979.

[18] S. Rouhani e E. Axelsson, «Calculation of Void Volume Fraction in the Subcooled and Quality Boiling Regions,» *International Journal of Heat and Mass Transfer,* vol. 13, pp. 383-393, 1970.

[19] A. Cavallini, J. S. Brown, D. Del Col e C. Zilio, «Intube condensation performance of refrigerants considering penalization terms (exergy losses) for heat transfer and pressure drop,» *International Journal of Heat and Mass Transfer,* vol. 53, 2010.

[20] A. Cavallini, D. Del Col, L. Doretti, M. Matkovic, L. Rossetto, C. Zilio e G. Censi, «Condensation in Horizontal Smooth Tubes: A New Heat Transfer Model for Heat Exchanger Design,» *Heat Transfer Engineering,* vol. 27, pp. 31-38, 2006.